Colloid Polym Sci 277:979–985 (1999)

ORIGINAL CONTRIBUTION

C.S. Chern
C.K. Lee
C.C. Ho

Electrostatic interaction between chitosan-modified latex particles and bovine serum albumin

Received: 26 March 1999
Accepted in revised form: 3 June 1999

C.S. Chern (✉) · C.K. Lee · C.C. Ho
Department of Chemical Engineering
National Taiwan University of Science and Technology
43 Keelung Road, Sec. 4
Taipei 106, Taiwan
e-mail: chern@ch.ntust.edu.tw
Fax: +886-2-27376644

Abstract Electrostatic interaction between poly(methyl methacrylate) latex particles with different levels of chitosan modification and bovine serum albumin (BSA) was investigated. The critical flocculation concentration is in the range 5–15 nmol dm^{-3} for these latex products toward added BSA. A series of isothermal equilibrium adsorption experiments shows that the adsorption process is divided into two distinct intervals. Adsorption of BSA on latex particles in intervals I and II is primarily controlled by charge neutralization and hydrophobic interaction, respectively. Intervals I and II can be reasonably described by an empirical parabola equation and the Langmuir isotherm model, respectively. The maximum amount of BSA adsorbed per unit weight of polymer particles was observed at pH ≅ 5. A maximum elution yield of about 80% can be achieved using NaSCN as the elution electrolyte, and NaSCN is more effective in inducing desorption of BSA from the particle surface than NaCl. The chitosan content has very little effect on the interaction between latex particles and BSA. By contrast, the influence of the content of 2,2′-azobis(2-amidinopropane) dihydrochloride, a cationic initiator used in preparing the chitosan-modified latex products, on the BSA adsorption process is significant.

Key words Bovine serum albumin · Chitosan-modified particles

Introduction

In our previous work, stable chitosan-modified polymethyl methacrylate (PMMA) latex particles were prepared using 2,2′-azobis(2-amidinopropane) dihydrochloride (V-50) as the cationic initiator [1]. Below pH 10.7, these submicron particles (with a very large particle surface area) carry positive charges and this characteristic makes them an attractive candidate for adsorbing negatively charged proteins, for example, bovine serum albumin (BSA) with pI = 4.8 [2], via electrostatic interaction, as reported by other researchers [3–6]. The preliminary data showed that colloidal stability plays an important role in the BSA adsorption process [1]. The colloidal system loses its stability as BSA adsorption proceeds. In addition to the self-promoting adsorption process provided by charge neutralization of latex particles by BSA [7, 8], the electrolyte (counterion) concentration is also expected to significantly affect their colloidal stability according to Deryagnin–Landau–Verwey–Overbeek theory [9, 10]. The flocculation rate and the floc structure have a significant impact on the binding capacity of latex particles.

To decouple the effects of ionic strength and charge neutralization, the influence of the NaCl (counterion Cl^-) concentration on the colloidal stability of these cationic latex particles was first investigated by experiments on coagulation kinetics [11]. The objective of this work is to focus on the electrostatic interaction between the chitosan-modified latex particles and BSA (a model protein). The electrolyte concentration is set at a level well below its critical coagulation concentration (CCC)

so that destabilization of the colloidal system primarily arises from charge neutralization. The results obtained from this series of studies may help us gain a better understanding of adsorption of proteins on these chitosan-modified latex particles.

Experimental

The latex products used in this work are PMMA latex particles with various levels of chitosan modification [1, 11]. For comparison, two chitosan-free latex products were included in this study. The free chitosan molecules and other impurities in the aqueous phase of the latex were removed according to the procedure developed in Ref. [11]. Some properties of these latex products are summarized in Table 1, in which [V-50] and [C] represent the weight percentages (based on total monomer) of V-50 and chitosan, respectively, used in the synthesis work. The parameters C_c and $C_{V\text{-}50}$ represent the weight percentages of chitosan and V-50 ultimately incorporated into the latex particles (based on PMMA weight). CCC(Cl^-) is the CCC of the latex sample at pH 7 toward NaCl. Other chemicals include BSA (98%, Sigma), sodium chloride (Acros), tris(hydroxymethyl) aminomethane (Acros), sodium acetate (Wako), acetic acid (Wako), sodium thiocyanate (Wako), hydrochloric acid (Wako), sodium hydroxide (Shimakyu), and deionized water (Barnsted, Nanopure Ultrapure Water System, specific conductance less than 0.057 μS/cm).

A typical isothermal equilibrium adsorption experiment is briefly described as follows. A latex sample was prepared using a pH 7 buffer solution of 2 mM tris(hydroxymethyl) aminomethane (ionic strength 1 mM Cl^-). The latex sample (2 ml) was then mixed with an equal volume of pH 7 tris(hydroxymethyl) aminomethane buffer solution comprising a prescribed amount of BSA to initiate adsorption of BSA on the particle surface. The reaction mixture with a particle solid content of 0.5% was stirred for 400 min at 25 °C. Approximately 98% of the equilibrium amount of BSA adsorbed was achieved within the first 5 min. The zeta potential (ζ) and particle size (d_p) of the latex sample taken immediately after the end of experiment were determined using a Zetamaster (Malvern) and a Photal LPA-3000/3100 (Otsuka), respectively. The ζ and d_p data represent an average of five and three measurements, respectively. The dilution water used for the measurements of ζ and d_p had the same ionic strength and pH as the latex sample. After centrifugation at 13 000 rpm for 10 min, the clear supernatant was filtered through a 0.2-μm membrane and the BSA concentration in the supernatant ([BSA]) was determined by the UV absorbance at 280 nm (Shimadzu UV-160 A).

To study the desorption of BSA from the particle surface, the precipitate obtained from the adsorption experiment was redispersed in pH 7 NaSCN (or NaCl) solution using a mini ultrasonic cleaner (Delta DG-1). The pH of the NaSCN (or NaCl) solution was adjusted using 0.1 N HCl and 0.1 N NaOH. This was followed by centrifugation of the latex sample at 13 000 rpm for 10 min. The clear supernatant was then filtered through a 0.2-μm membrane, and [BSA] was determined by UV absorbance at 280 nm.

Table 1 Some physical properties of the poly(methyl methacrylate) latex particles with various levels of chitosan modification taken from Refs. [1, 11]

Latex	I5	I50	C1	C20
[V-50] (%)	0.05	0.5	0.5	0.5
[C] (%)	–	–	0.1	2
d_w (nm)	309	262	245	232
$C_{V\text{-}50}$ (%)	0.8	8.3	8.3	8.3
C_c (%)	–	–	0.08	1.7
Critical coagulation concentration (Cl^-) (mmol dm^{-3})	50	60	37	33

Results and discussion

First, experiments on coagulation kinetics [12, 13] were used to determine the critical flocculation concentration of latex particles toward BSA [CFC(BSA)], but this attempt was not successful. The ζ and d_p data for latex products I5, I50, and C20 (2 mM NaCl, pH 7 adjusted using 0.1 N HCl and 0.1 N NaOH) as a function of the initial BSA concentration in the aqueous phase ($[BSA]_0$) are shown in Figs. 1 and 2, respectively. In this series, the ionic strength (2 mM Cl^-) is well below the CCC(Cl^-) data shown in Table 1. The value of ζ (or particle surface charge density) first remains relatively constant and then decreases rapidly with increasing $[BSA]_0$ due to charge neutralization of the positively charged particles by negatively charged BSA molecules. This is followed by the reversal of particle surface net charge (from positive to negative) at high $[BSA]_0$. Figure 2 shows three distinct intervals:

1. d_p first remains relatively constant with $[BSA]_0$, which reflects a quite stable colloidal system involved in the adsorption process.

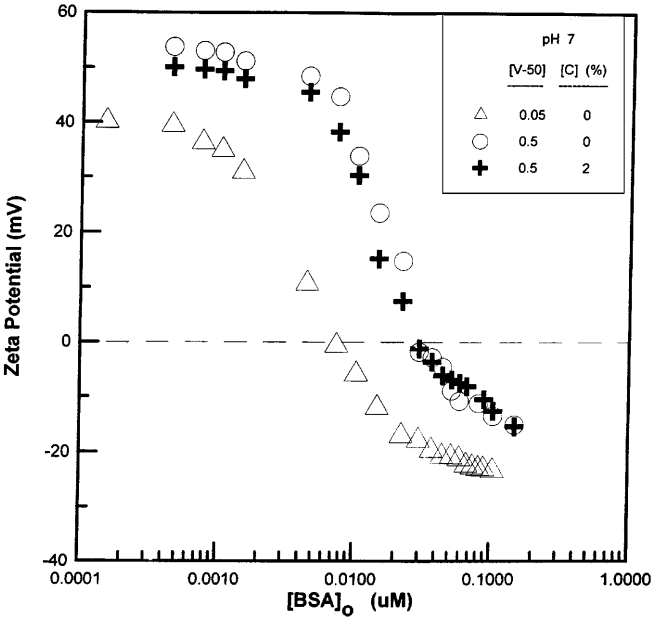

Fig. 1 Profiles of zeta potential versus initial bovine serum albumin (BSA) concentration in the aqueous phase for the latex sample at pH 7 taken immediately after the end of the isothermal equilibrium adsorption experiment. I5 (△); I50 (○); C20 (✚)

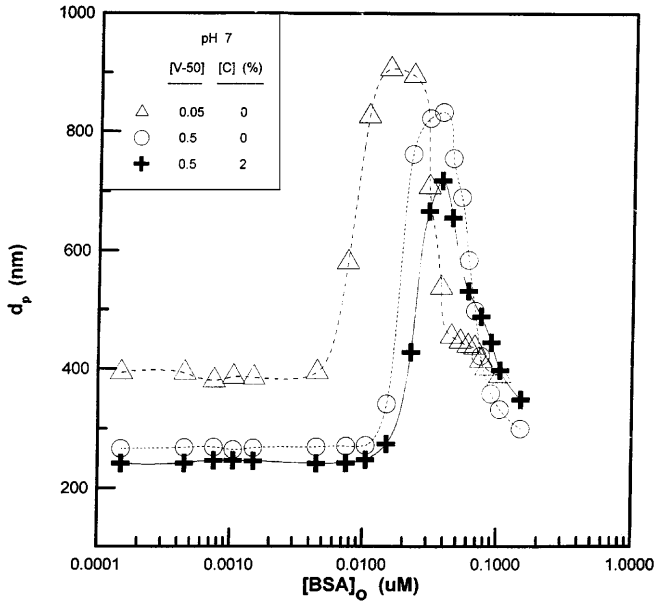

Fig. 2 Profiles of particle size versus initial BSA concentration in the aqueous phase for the latex sample at pH 7 taken immediately after the end of the isothermal equilibrium adsorption experiment. I5 (△); I50 (○); C20 (✚)

2. d_p increases rapidly to a maximum due to the greatly enhanced flocculation.
3. d_p then decreases rapidly as a result of restabilization of latex particles.

Such a d_p versus $[BSA]_0$ profile is closely related to the ζ data in Fig. 1, i.e., the larger the absolute value of ζ, the greater the colloidal stability.

It is interesting to note that [V-50] has a significant influence on both ζ and d_p (see I5 and I50 in Figs. 1, 2). The higher the [V-50], the greater the particle surface charge density (i.e., the more stable the colloidal system). At constant $[BSA]_0$, ζ and d_p for I50 and C20, however, do not vary significantly. One possible explanation is that the initial particle size of C20 (d_w = 232 nm, Table 1) is smaller than that of I50 (d_w = 262 nm), i.e., the total particle surface area of C20 per unit weight of polymer particles is larger than that of I50. Nevertheless, the C20 latex particles carry more electric charges ($C_{V\text{-}50}$ = 8.3% and C_c = 1.7%, Table 1) than I50 ($C_{V\text{-}50}$ = 8.3% and C_c = 0%). Thus, the particle surface charge density (i.e., ζ) of C20 is quite close to that of I50. Another contributing factor is that chitosan grafted onto the C20 particle surface will shift the shear plane toward the aqueous solution and, thereby, reduce the ζ of the latex particles. On the other hand, chitosan contributes to particle surface charge density and, thereby, increases the ζ of the latex particles. It is postulated that all these factors lead to the insignificant effect of [C] on the ζ and d_p data as a function of $[BSA]_0$. CFC(BSA), defined as the point at which d_p increases sharply with $[BSA]_0$ in Fig. 2, was estimated to be 4.7, 11.2, and 14.5 nmol dm^{-3} for I5, I50, and C20, respectively. These data indicate that colloidal stability increases with increasing [V-50]. Chitosan provides latex particles with additional steric stabilization, thereby promoting the colloidal stability of C20 compared to I50. In addition, CFC(BSA) is several orders of magnitude smaller than CCC(Cl^-). This implies that charge neutralization of latex particles by BSA is the primary destabilization mechanism.

The Langmuir isotherm model [14–16] has been widely used to describe the equilibrium adsorption of protein (e.g., BSA) on the particle surface:

$$q^* = q_{max}c^*/(K_d + c^*) \quad (1)$$

or

$$q^* = q_{max} - K_d q^*/c^* \ , \quad (2)$$

where q^* is the amount of BSA adsorbed per gram of polymer particles, q_{max} is the maximum amount of BSA that can be adsorbed on the particle surface, c^* is the BSA concentration in the aqueous solution, and K_d is the dissociation constant for the BSA-binding-site pair. Thus, K_d and q_{max} can be obtained from the slope and intercept, respectively, of the Scatchard plot of the Langmuir adsorption isotherm (see Eq. 2).

Figures 3–5 show adsorption isotherm curves and Scatchard plots for BSA adsorbed on I5, I50, C1, and C20 latex particles at pH = 4.8, 7.0, and 9.0, respectively. Similar q^* versus c^* profiles are observed for latex products. The adsorption isotherm is empirically divided into two distinct intervals, i.e., q^* first increases sharply with increasing c^* (interval I) and then levels off (interval II). The q^* versus q^*/c^* data in interval I do not follow Eq. (1) and a partial parabola seems to describe the experimental data reasonably well. At relatively low c^* (e.g., $c^* < 1$ μmol dm^{-3} and $q^* < 0.25$ μmol g^{-1} for C20 at pH 7 in Fig. 3), the rapidly increased q^* with c^* is attributed to intensive flocculation of positively charged latex particles by adsorption of negatively charged BSA. The number of effective binding sites on the particle surface may be greatly reduced owing to the steric hindrance effect provided by formation of flocs. The variations of the particle surface binding sites in a series of isothermal equilibrium adsorption experiments (interval I) may thus result in a significant deviation from the Langmuir isotherm model. Neglecting the influence of the type of electrolytes used, the ζ and d_p data in Figs. 1 and 2, respectively, may help provide an insight into the adsorption mechanisms involved. The ratio of the number of BSA molecules to the number of latex particles initially added to the system (B/P) calculated at various conditions can be found in Table 2. At pH 7, the values of B/P determined at the turning point of the q^* versus q^*/c^* data in Fig. 4b are located between those calculated at CFC(BSA) and the maxi-

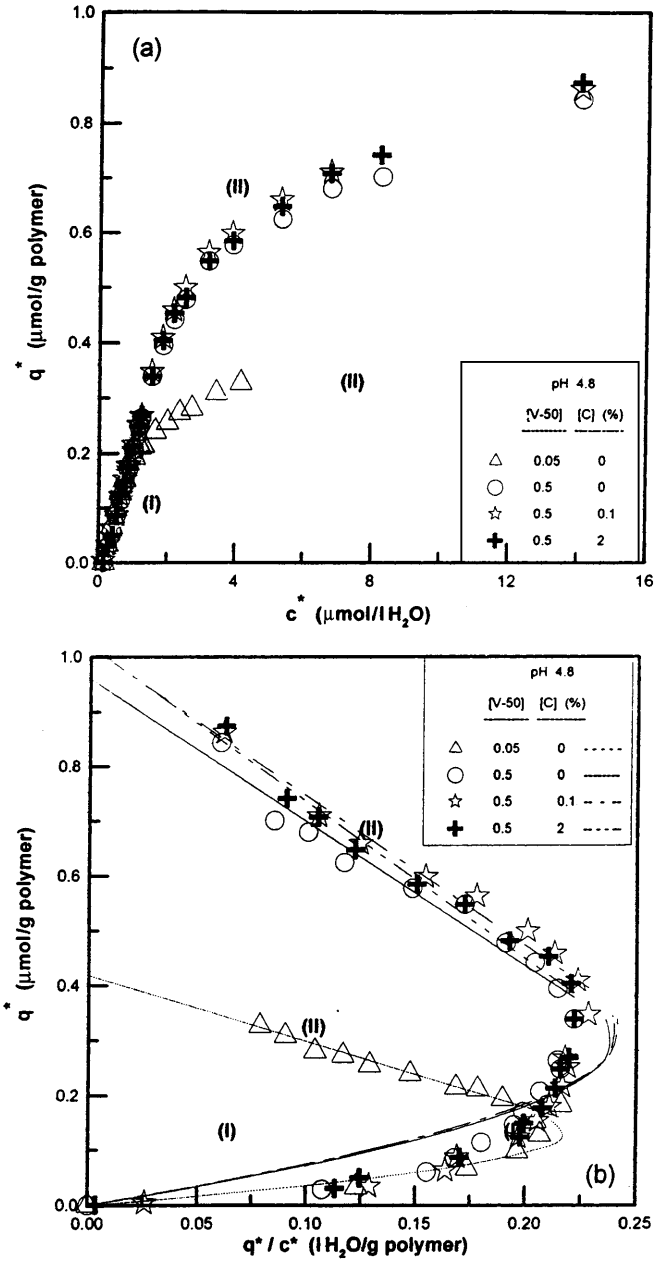

Fig. 3 **a** Langmuir isotherm curves and **b** Scatchard plots for BSA adsorbed on latex particles at pH 4.8. I5 (△); I50 (○); C1 (☆); C20 (✚)

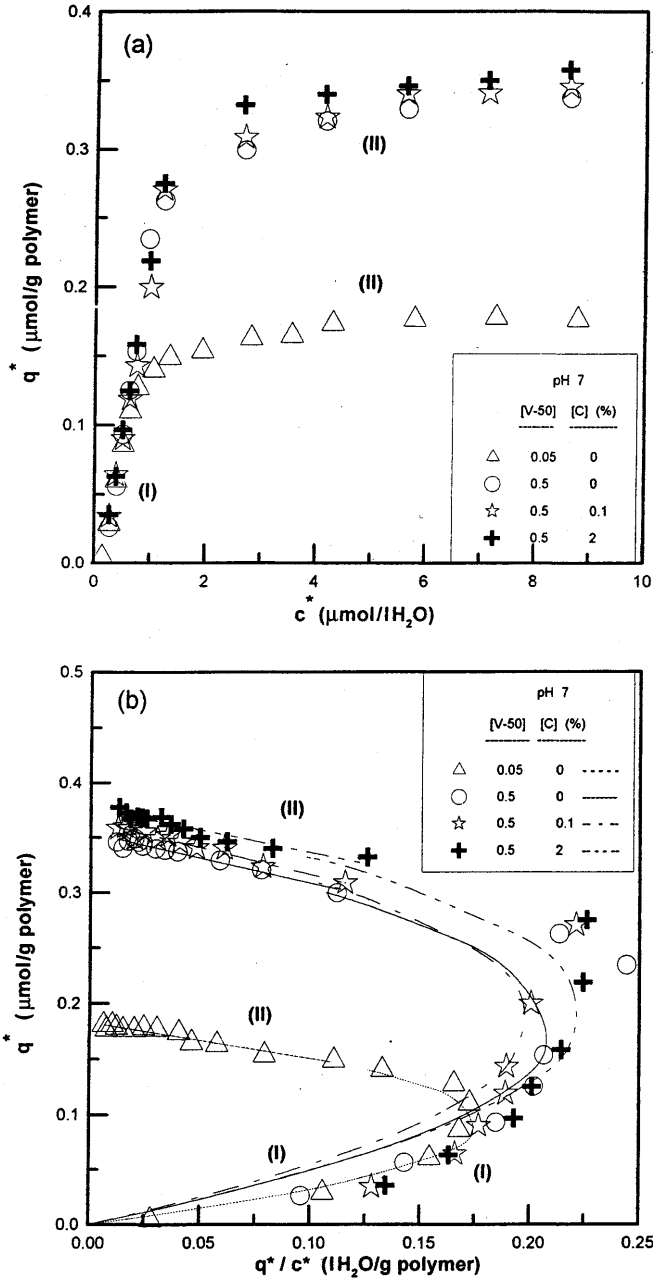

Fig. 4 **a** Langmuir isotherm curves and **b** Scatchard plots for BSA adsorbed on latex particles at pH 7. I5 (△); I50 (○); C1 (☆); C20 (✚)

mum d_p in Fig. 2. This indicates that significant flocculation of positively charged latex particles by adsorption of negatively charged BSA species must have occurred in interval I. At pH 4.8 and 7, the initial slope of the q^* versus c^* curve for I5 is comparable to those for I50, C1, and C20 (see Figs. 3a, 4a). In contrast, at pH 9 the initial slope of the q^* versus c^* curve for I5 is smaller than those for I50, C1, and C20 (Fig. 5a). This is attributed to the fact that the ζ of the latex particles first remains relatively constant and then decreases rapidly with increasing pH (2–10.7) [1]. This characteristic is then reflected in the electrostatic interaction between the latex particles and the approaching BSA molecules.

Further increasing c^* leads to a transitional region in which reversal of particle surface charge (from positive to negative) takes place. Nevertheless, the particle surface charge density may not be high enough to assure a stable colloidal system and, perhaps, mixed modes of adsorption mechanisms (electrostatic and hydrophobic interactions) are responsible for the BSA adsorption process

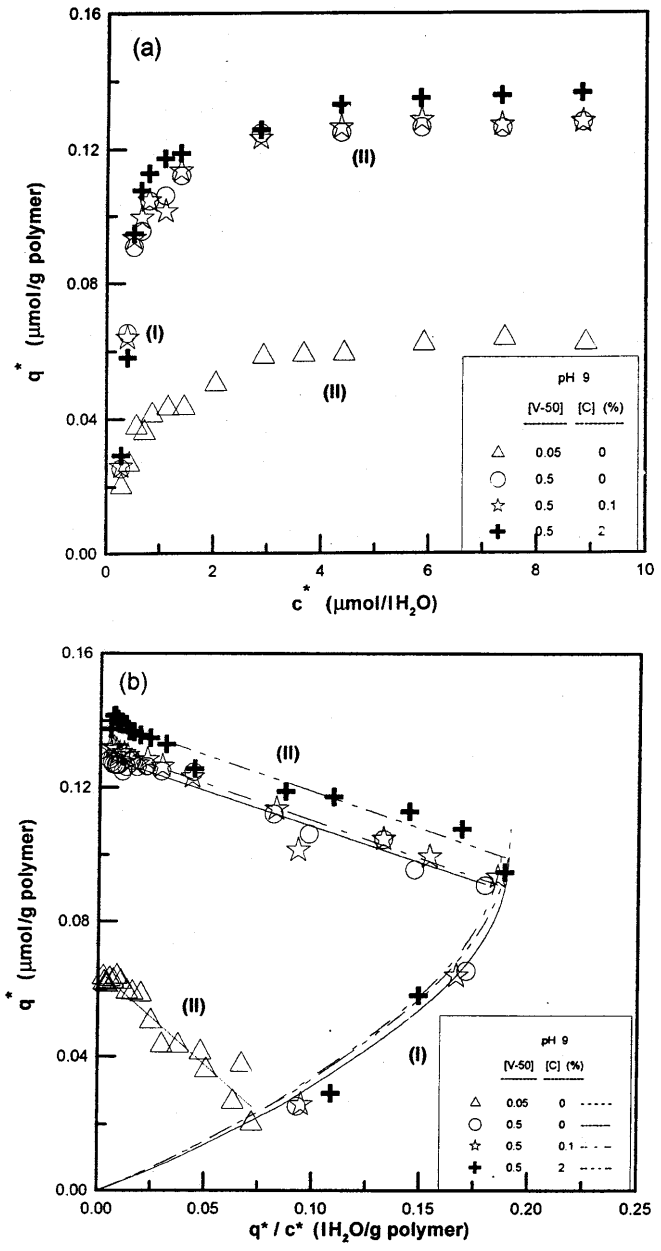

Fig. 5 **a** Langmuir isotherm curves and **b** Scatchard plots for BSA adsorbed on latex particles at pH 9. I5 (△); I50 (○); C1 (☆); C20 (✚)

Table 2 Ratio of bovine serum albumin (BSA) molecules to latex particles initially added to the system calculated at various conditions in interval I

Latex	$B/P \times 10^{-16}$		
	I5	I50	C20
At critical flocculation concentration (BSA), pH 7 (Fig. 2)	2.83	6.75	8.73
At maximum d_p, pH 7 (Fig. 2)	8.99	17.98	22.47
At turning point, pH 7 (Fig. 4b)	7.19	10.79	14.38

in this transitional region. At still higher c^* (e.g., $c^* > 1$ μmol dm^{-3} and $q^* > 0.25$ μmol g^{-1} for C20 at pH 7 in Fig. 3), the colloidal system is restabilized because of the greatly enhanced particle surface charge density during interval II. Adsorption of BSA onto the latex particles is thus primarily controlled by hydrophobic interaction in this interval. Ortega-Vinuesa and Hidalgo-Alvarez [17] pointed out that adsorption of protein occurs spontaneously even when the protein has the same charge sign as the particle surface. In this case, adsorption of BSA is due to the attractive interaction between hydrophobic PMMA patches on the particle surface and hydrophobic regions on the BSA surface. In interval II, the slope of q^* versus c^* gradually decreases with increasing c^* and then levels off due to the decreased number of particle surface binding sites, the increased electrostatic repulsion force between two adjacent BSA molecules adsorbed on the particle surface, and the enhanced electrostatic repulsion force between latex particles and the approaching BSA species. As a consequence, the q^* versus q^*/c^* data can be described by the Langmuir isotherm model. The ζ of the latex particles with various levels of chitosan modification is about −20 mV when the equilibrium amount of adsorbed BSA is achieved. This provides supporting evidence for the proposed adsorption mechanism in interval II. It is also interesting to note that interval I is not observed for the run with I5 at pH 9. The adsorption system follows the Langmuir isotherm model, although the triangular data points in Fig. 4b are somewhat scattered. This is most likely due to the fact that I5 has the lowest particle surface charge density and it only require a very small amount of BSA to induce flocculation. In this series of isothermal equilibrium adsorption experiments, the colloidal system undergoes restabilization, thereby leading to the Langmuir adsorption isotherm.

Equation (2) and the following empirical equation proposed by Suen [18] were used to fit the q^* versus q^*/c^* data in intervals I and II:

$$q^*/c^* = q_{max}/K_d q^* - 1/K_d q^{*2} \quad . \tag{3}$$

The q_{max} and K_d data determined by the least-squares best-fit method are summarized in Table 3, where r^2 is the coefficient of determination. At constant pH, q_{max} increases with increasing [V-50] because the number of particle surface -NH_3^+ groups increase with $C_{V\text{-}50}$ (see I5 and I50 in Tables 1, 2); however, C_c seems to have little effect on q_{max} (see I50, C1, and C20 in Tables 1, 2). Such insignificant influence of C_c is also observed for the ζ and d_p data in Figs. 1 and 2 and those results presented in our previous work [1, 11]. Furthermore, for a particular latex, q_{max} decreases with increasing pH due to the reduced degree of protonation of the particle surface -NH_2 groups with pH (see Table 3). The lower the particle surface charge density, the smaller the

Table 3 Maximum amounts of adsorbed BSA and dissociation constants for latex particles with various levels of chitosan modification

Latex	I5	I50	C1	C20
Interval I				
pH 4.8 q_{max} (μmol g^{-1})	0.263	0.604	0.629	0.412
K_d (μmol dm^{-3})	0.080	0.381	0.410	0.412
r^2	0.998	0.952	0.955	0.942
pH 7 q_{max} (μmol g^{-1})	0.183	0.352	0.365	0.380
K_d (μmol dm^{-3})	0.048	0.148	0.167	0.161
r^2	0.981	0.832	0.819	0.871
pH 9 q_{max} (μmol g^{-1})	–	0.198	0.209	0.213
K_d (μmol dm^{-3})	–	0.051	0.058	0.059
r^2	–	0.950	0.840	0.931
Interval II				
pH 4.8 q_{max} (μmol g^{-1})	0.424	0.946	0.998	1.003
K_d (μmol dm^{-3})	1.250	2.496	2.565	2.709
r^2	0.969	0.964	0.985	0.982
pH 7 q_{max} (μmol g^{-1})	0.183	0.354	0.365	0.377
K_d (μmol dm^{-3})	0.323	0.456	0.488	0.406
r^2	0.938	0.956	0.962	0.909
pH 9 q_{max} (μmol g^{-1})	0.065	0.129	0.133	0.140
K_d (μmol dm^{-3})	0.556	0.198	0.292	0.214
r^2	0.933	0.945	0.940	0.944

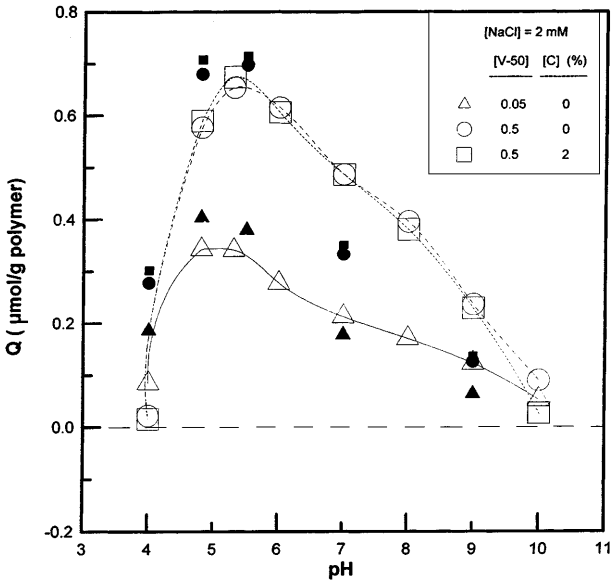

Fig. 6 Effect of pH on the amount of BSA ultimately adsorbed on latex particles. I5 (△, ▲); I50 (○, ●); C20 (□, ■). The *open data points* represent the experiment with 2 mM NaCl and different pH values adjusted using NaOH and HCl. The *closed data points* represent the experiment with different pH values adjusted using 2 mM tris(hydroxymethyl) aminomethane buffer

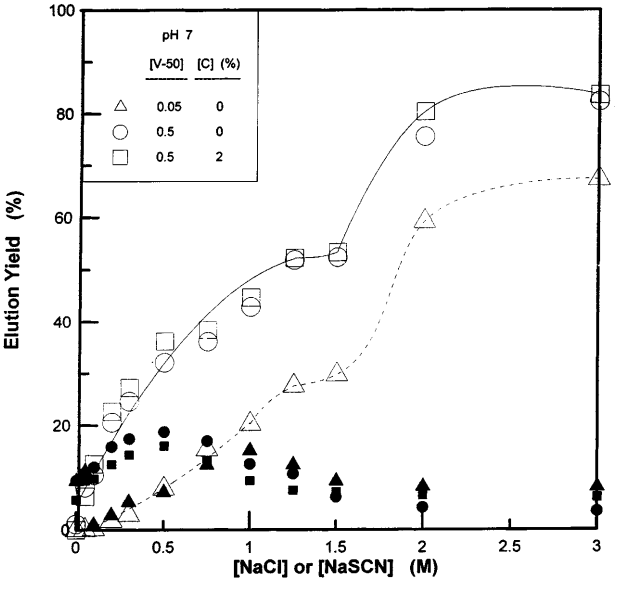

Fig. 7 Effect of NaCl or NaSCN concentration on the elution yield of BSA at pH 7. I5 (△, ▲); I50 (○, ●); C20 (□, ■). The *open data points* represent the experiment with NaSCN as the elution electrolyte. The *closed data points* represent the experiment with NaCl as the elution electrolyte

amount of BSA which can be adsorbed onto the latex particles. Similar trends are also observed for the dependence of K_d on such parameters as $C_{V\text{-}50}$, C_c, or pH in interval I, in which charge neutralization plays an important role in the adsorption process; however, no apparent correlation between K_d and $C_{V\text{-}50}$, C_c, or pH is observed for interval II, in which both latex particles and BSA carry net negative charge and adsorption of BSA is achieved by hydrophobic interaction (Tables 1, 2).

The effect of pH on the amount of BSA adsorbed per unit weight of PMMA (Q) is shown in Fig. 6. Q seems to be not very sensitive to the type of electrolytes used in this series of experiments. The maximum Q occurs at pH $\cong$ 5. This is because BSA possesses more negative charges and the ζ of the latex particles is lower when the pH increases from 5 (close to the isoelectric point of BSA, 4.8) to 10. Therefore, the positively charged latex particles can adsorb (or neutralize) fewer BSA molecules. In addition, the net negative charges on the BSA surface increase with increasing pH, thereby leading to a reduction in the conformational stability of BSA. This then results in structural rearrangements of adsorbed BSA and a larger surface area per BSA molecule and, consequently, the decreased Q with pH is observed [19]. When the pH decreases from 5 to 4, the electrostatic repulsion force between positively charged latex particles and BSA increases. This will result in a decrease in Q.

The influence of NaCl or NaSCN concentration ([NaCl] or [NaSCN]) on the elution yield of adsorbed BSA at pH 7 is shown in Fig. 7. It is shown that the elution yield first increases to a maximum (about 10–20%) and then decreases with increasing [NaCl] (see the closed data points in Fig. 7). It is postulated that increasing [NaCl] compresses the electric double layer of the latex particles, reduces the electrostatic interaction

between latex particles and BSA, and, thereby, results in desorption of BSA from the particle surface. Upon further increasing [NaCl] to a level above its CCC(NaCl) (30–60 mM, Table 1), however, the desorbed BSA molecules may be trapped within the flocs formed and they become incapable of diffusing out of the cage. Besides, BSA exposed to an aqueous environment with high ionic strength may diffuse back to the hydrophobic patches on the particle surface and, again, adsorb onto the particle surface due to the salting-out effect. These factors cause a decrease in the elution yield with increasing [NaCl]. By contrast, the elution yield first increases and then reaches a plateau (about 70–80%) when [NaSCN] increases from 0 to 3 M (see the open data points in Fig. 7). The absence of a maximum in the elution yield versus [NaSCN] curve is due to the fact that

1. SCN^- is less effective in inducing coagulation of latex particles than Cl^- [20].
2. The hydrophobic interaction between latex particles and BSA in the SCN^- medium and the dehydration power of SCN^- are smaller than the Cl^- counterpart [21].

Finally, it should be noted that both Q and elution yield are insensitive to C_c (I50 versus C20) but are dependent on $C_{V\text{-}50}$ (I5 versus I50), as shown in Figs. 6 and 7.

References

1. Chern CS, Lee CK, Ho CC (1999) J Polym Sci Polym Chem Ed 37:1489
2. Yoshida H, Nishihara H, Kataoka T (1994) Biotechnol Bioeng 43:1087
3. Kim CW, Kim SK, Rha CK (1987) In: Attia YA (ed) Flocculation in biotechnology and separation systems. Elsevier, Amsterdam, p 467
4. Kim CW, Rha CK (1989) Biotechnol Bioeng 33:1205
5. Ortega-Vinuesa JL, Hidalgo-Alvarez R (1994) J Biomater Sci Polym Ed 6:269
6. Ortega-Vinuesa JL, Hidalgo-Alvarez R (1995) Biotechnol Bioeng 47:633
7. Shubin V, Samoshina Y, Menshikova A, Evseeva T (1997) Colloid Polym Sci 275:655
8. Chern CS, Lee CK, Tsai YJ, Ho CC (1998) Colloid Polym Sci 276:427
9. Deryagnin BV, Landau LD (1941) Acta Physicochim URSS 14:633
10. Verwey EJW, Overbeek JThG (1943) Theory of the stability of lyophobic colloids. Elsevier, New York
11. Chern CS, Lee CK, Ho CC (1999) Colloid Polym Sci
12. Tsaur SL, Fitch RM (1987) J Colloid Interface Sci 115:463
13. Carrique F, Salcedo J, Cabrerizo MA, Gonzalez-Caballero F, Delgado AV (1991) Acta Polym 42:261
14. Belter PA, Cussler EL, Hu WS (1988) Bioseparations, downstream processing for biotechnology. Wiley, New York
15. Scatchard G (1949) Ann NY Acad Sci 51:600
16. Price NC, Lewis S (1982) Fundamentals of enzymology. Oxford University Press, Oxford
17. Ortega-Vinuesa JL, Hidalgo-Alvarez R (1995) Biotechnol Bioeng 47:633
18. Suen SY (1997) J Chem Technol Biotechnol 70:278
19. Elgersma AV, Zsom RLJ, Norde W, Lyklema J (1991) J Colloid Interface Sci 138:145
20. Hiemenz PC (1985) Principles of colloid and surface chemistry, 2nd edn, Dekker, New York
21. Suzawa T, Shirahama H (1991) Adv Colloid Interface Sci 35:139